

Published in final edited form as:

Talanta. 2010 September 15; 82(4): 1149–1155. doi:10.1016/j.talanta.2010.06.025.

Oxidation and flow-injection amperometric determination of 5-hydroxytryptophan at an electrode modified by electrochemically assisted deposition of a sol-gel film with templated nanoscale pores

David Ranganathan^{a,b}, Silvia Zamponi^b, Mario Berrettoni^c, B. Layla Mehdi^a, and James A. Cox^{a,*}

^a Department of Chemistry and Biochemistry, Miami University, Oxford, Ohio 45056, USA

^b Department of Chemical Science, University of Camerino, Via S. Agostino 1, 62032 Camerino, Italy

^c Department of Physical and Inorganic Chemistry, University of Bologna and Unità di Ricerca, INSTM di Bologna, Viale Risorgimento 4, 40136, Bologna, Italy

Abstract

The oxidation of 5-hydroxytryptophan (5-HTPP) yielded a passivating polymeric film at an indium tin oxide (ITO) electrode. Coating ITO with a nanoscale sol-gel film with a mesoporous structure was shown to change the pathway of the chemical reaction coupled to the electron transfer. The sol-gel film was deposited by an electrochemically assisted process, and the mesoporosity was imparted by including generation-4 poly(amidoamine) dendrimer in the precursor solution. The dendrimer was removed subsequently with an atmospheric oxygen plasma. This electrode remained active during cyclic voltammetry and controlled potential electrolysis of 5-HTPP, which was attributed to dimer, rather than polymer, formation from the oxidation product. Mass spectrometry confirmed this hypothesis. The anodic current was limited by the electron-transfer kinetics. Modification of the sol-gel film by inclusion of cobalt hexacyanoferrate, which catalyzes the oxidation, resulted in a diffusion-limited current. Determination of 5-HTPP by flow-injection amperometry had a detection limit of 17 nM.

Keywords

Sol-gel films; Electrochemically assisted deposition; 5-Hydroxytryptophan; Voltammetry; Flow injection analysis

1. Introduction

Electroanalytical measurements in real-world samples are often hindered or precluded by adsorption of matrix components, of the analyte and/or of the products of the electron-transfer reaction. In the common case of passivation by matrix components, an approach to circumventing this limitation is to modify the electrode with a film that is permeable to the

*Corresponding author, Tel. 1 513 529 2493; fax 1 513 529 5715, coxja@muohio.edu.

Publisher's Disclaimer: This is a PDF file of an unedited manuscript that has been accepted for publication. As a service to our customers we are providing this early version of the manuscript. The manuscript will undergo copyediting, typesetting, and review of the resulting proof before it is published in its final citable form. Please note that during the production process errors may be discovered which could affect the content, and all legal disclaimers that apply to the journal pertain.

analyte but blocks transport of concomitants. Perhaps the first report of this electrode design was by Sittampalam and Wilson [1] who used hydrolyzed cellulose acetate (CA) as the barrier in an amperometric method for the determination of hydrogen peroxide in a complex matrix. Here, the pore size permitted facile diffusion of the analyte but was smaller than the size of the surface-active matrix components. The use of CA as the electrode modifier has several limitations including inability to dope the material with a catalyst, inexact control of pore size and film thickness, and limited physical stability. To overcome such limitations of CA and to explore other potential attributes of nanoporous domains for electrochemical reactions, we are investigating the modification of electrodes with nanometer-scale, mesoporous sol-gel films [2].

The method for preparing sol-gel films in the present study is based on recent reports of their electrochemically assisted formation. A common sol-gel process consists of the hydrolysis, condensation and polycondensation of a tetraalkylorthosilicate to form microporous or mesoporous silica. This process is initiated and sustained by changing the near-neutral pH of a stable precursor sol to an acidic or basic value at which sol-gel processing is catalyzed. Conventional sol-gel processing is used to produce a variety of geometries such as monoliths and micron-scale cast or spin-coated films. In electrochemically assisted methods [3–6], electrolysis of water in quiescent, unbuffered sol generates an acidic (at positive potentials) or basic (at negative potentials) environment exclusively at the electrode-liquid interface. Mandler and co-workers [4–6] initiated this process by applying a potential sufficient to electrolyze water to an electrode immersed in an electrolyte that contained a sol-gel precursor, zirconium-tetra-n-propoxide [5]; a typical electrolysis time was 15 min. The film thickness was varied intentionally over the range from tens of nanometers to ca. 1000 nm. The thickness achieved depended on such factors as the applied potential, the nature of the electrode material, and the water content of the supporting electrolyte. In concert, these factors varied the rate of change of interfacial pH that, in turn, controls the rates of condensation and of polycondensation. The sol-gel films prepared in this manner are highly resistive; therefore, they are well-suited to corrosion protection.

A variation of the procedure, namely the inclusion of β -cyclodextrin (CD) in the precursor solution, yielded porous films that maintained the electrochemical activity of the substrate [2]. An indium tin oxide (ITO) electrode was coated with silica by applying 2.35 V vs. a Pt quasi-reference electrode for 30 min in a solution comprising 2-propanol as the bulk liquid-phase, lithium perchlorate as the supporting electrolyte, water to serve as the proton source upon electrolysis, CD as the templating agent, and tetraethylorthosilicate (TEOS) as the sol-gel precursor. The resulting film-coated ITO electrode was withdrawn from the plating bath at $50 \mu\text{m}\cdot\text{min}^{-1}$ to provide controlled drainage of the liquid from the electrode surface. The vertical stacking of CD on the electrode [7] resulted in the formation of a sol-gel film with controlled porosity. For the voltammetric determination of phospholipids, the composite of CD and sol-gel was doped with bis(acetate)dirhodium-11-molybdophosphate, which is an oxidation catalyst [8], by inclusion of this complex in the precursor solution. At this modified electrode, the oxidation of phosphatidylcholine (PC) was observed by cyclic voltammetry, and the anodic current persisted during repeated potential scans. In contrast, at bare ITO the adsorption of PC passivated the electrode. Evidence was that the oxidation of a test species, 1.0 mM ferrocene, was blocked when 100 μM PC was present [2].

Walcarius et al. [3] described an approach to electrochemically assisted deposition of sol-gels that yielded nm-scale mesoporous films with pores perpendicular to the electrode surface. The procedure combined base-catalyzed sol-gel processing of tetraethylorthosilicate (the pH was locally increased at the electrode surface by electrochemical reduction of hydronium and water in unbuffered solution) with orientation of channels in

cetyltrimethylammonium bromide (CTAB) assembled in hemi-micelles at the electrode surface by the electric field. The films were characterized after dissolution of the CTAB. They exhibited high pore density ($75,000 \text{ pores} \cdot \mu\text{m}^{-2}$) and pore volume. The diffusion coefficient of ferrocene ethanol, $3.5 \times 10^{-6} \text{ cm}^2 \cdot \text{s}^{-1}$, in these films demonstrated its facile mobility therein.

Pore size of a sol-gel matrix has been shown to influence the pathway of electrochemical reactions performed therein. The electrochemical oxidation of an aniline as a dopant in a microporous silica sol-gel [9] and in a mesoporous organically modified sol-gel [10] was investigated. The primary product was a dimer in the former and a polymer in the latter, which is a result consistent with a restriction of the size of the product of a chemical reaction following electron transfer in a microporous domain. The sol-gel matrix can affect reaction pathways by means other than pore size. For example, UO_2^+ formed by the electrochemical reduction of UO_2^{2+} in a silica sol-gel monolith rapidly disproportionated whereas UO_2^+ was stable when the reduction UO_2^{2+} was at an electrode immersed in aqueous solution [11]. Catalysis of the disproportionation reaction was related to the ion-exchange reaction between the UO_2^+ and the negative sites of the silica. Interactions with sol-gel matrices influence other types of reactions as well. For example, hydrogen bonding of the starting compound with silanol sites catalyzed the photochemical conversion of *trans*-4-methoxy-4'-(2-hydroxyethoxy)-azobenzene to the *cis* configuration [12].

The present study is an extension of preliminary work on the analytical utility of sol-gel films with controlled porosity as electrode modifiers. The initial study employed films that were doped with a redox mediator (a Rh^{II} complex) and had pores templated with CD, which has a toroid structure with a 7-nm cavity. Because the pores were smaller than the size of the analyte, the mediated oxidation occurred at the interface of the Rh^{II} -doped sol-gel film and the electrolyte solution that contained the analyte [2]. This study focused on an analyte that was small enough to diffuse through the pores to the electrode surface. The test species that was selected, 5-hydroxytryptophan (5-HTPP), had been shown previously to undergo chemical oxidation by a pathway that was influenced by pore size of the matrix [13]. When the 5-HTPP was a component of a microporous silica sol-gel monolith, chemical oxidation resulted in dione formation whereas dimer was formed in mesoporous silica. The voltammetry of 5-HTPP in a silica sol-gel monolith was investigated at a boron-doped diamond electrode [14]; however, passivation of the electrode precluded generation of sufficient product for identification. The gradual passivation of the working electrode surface during the oxidation of 5-HTPP was mitigated by the use of a catalyst such as a Ru^{II} metallo dendrimer incorporated into a carbon composite [15]. For the present study, cobalt hexacyanoferrate (CoHCF) was selected because it has been reported to catalyze the oxidation of substrates related to 5-HTPP, including tryptophan, and it is convenient to prepare at the surface of electrodes [16].

Because our previous study showed a difference between microporous and mesoporous silica matrices in terms of the pathway of 5-HTPP oxidation [13], amine-terminated generation 4-polyamidoamine dendrimer (PAMAM), which has a calculated sphere diameter of 4.5 nm [17], was used rather than CD to template the pore size. An additional reason for the choice of PAMAM was that these dendrimers have a diameter that depends on generation in a known manner [18], so successful fabrication of porous sol-gel films in the present study can be applied to future investigations on the role of pore size on the voltammetric behavior of a variety of analytes.

2. Material and methods

Potassium ferricyanide, potassium chloride, monobasic potassium phosphate, dibasic potassium phosphate, cobalt chloride, ethanol, acetonitrile, sodium nitrate, and hydrochloric acid were ACS Reagent Grade from Fisher Scientific (Fair Lawn, NJ). The 5-HTPP was from Sigma (St. Louis, MO). The following were obtained from Aldrich (Milwaukee, WI): tetraethylorthosilicate (TEOS), amine-terminated generation 4-polyamidoamine (PAMAM), 98% purity; α -cyano-4-hydroxycinnamic acid (CHCA), 97% purity; and CTAB. Water used in this study was house-distilled that was further purified with a Barnstead NANO pure II system.

Electrochemical experiments were performed on CH Instruments (Austin, TX) Models 400, 660B or 800 electrochemical workstations. The working electrode was indium tin oxide (ITO) from Delta Technologies (Stillwater, MN). The ITO was rinsed with ethanol, dried under nitrogen, and cut into squares with 1.5 cm edges prior to use as electrodes. Using a rubber o-ring, a 0.32 cm² portion of this ITO was isolated as the working electrode. All potentials were measured and reported against an Ag|AgCl, 3 M KCl reference electrode (Bioanalytical Systems, West Lafayette, IN). The counter electrode was platinum gauze. The matrix-assisted laser desorption/ionization mass spectrometry (MALDI) experiments were performed with a Bruker Ultraflex III instrument with a time-of-flight mass analyzer (Billerica, MA).

The flow injection amperometry (FIA) experiments were performed with a system comprised of a 30-mL syringe pump (Pharmaseal Laboratories, Glendale, CA), Rhyodyne 7010loop injector, and a thin layer electrochemical cell (Bioanalytical Systems, West Lafayette, IN). The cell with a Pt auxiliary electrode and a Ag|AgCl reference electrode was modified to incorporate a sol-gel coated ITO (0.32 cm²) working electrode.

Mesoporous silica sol-gel films were deposited on the ITO electrodes under potentiostatic conditions adapted from Walcarius et al. [3]. A typical precursor solution consisted of 13.6 mmol TEOS, 10 mL ethanol, 10 mL 0.1 M NaNO₃ (aqueous), 1.0 mM PAMAM, and 1.0 mM HCl (aqueous), to which 4.35 mmol CTAB was added while stirring. The pH was adjusted to 3.0 with dilute HCl. The CTAB/TEOS ratio was maintained at 0.32; under this condition highly ordered pores were obtained [3]. The solution was aged for 120 min under stirring prior to introduction of the ITO electrode. Deposition of a sol-gel film on the ITO was achieved by applying a cathodic potential that was sufficiently negative to reach the onset of water reduction. Generally, the reduction was done at -1.8 V for 10 s. The electrode was rapidly removed from the solution and immediately rinsed with water to avoid additional sol-gel formation by a chemical process. This surfactant-templated film was dried and aged overnight. The CTAB and the PAMAM were removed from the ITO|sol-gel prior to its use as an electrode. The initial step was treatment with an oxygen plasma using a March Plasma Systems (Concord, CA) device. Subsequently, the electrode was soaked for 3 h in a mixture prepared with equal volumes of ethanol and 0.1 M HCl (aqueous). Unless otherwise stated, the resulting sol-gel coated electrode with nm-scale pores in the sol-gel, designated as ITO|npSG, was used in all experiments. In some cases the ITO|npSG was modified with CoHCF. The procedure was adapted from a previous report [19]. The electrode was immersed for 60 min in 0.01 M CoCl₂. After rinsing with water, it was immersed in 0.01 M K₃Fe(CN)₆ for 60 min.

3. Results and discussion

3.1. Fabrication and characterization of the sol-gel film

The goal of the study was to synthesize and apply a sol-gel film with a controlled pore size on electrode surfaces by using PAMAM as a templating agent. A concern was that the presence of PAMAM in the sol-gel film will interfere with the electrochemical behavior; therefore, removal of the PAMAM by exposure of the modified electrode to an oxygen plasma was evaluated. The plasma was operated at 100 W and 0.3 Torr, and the time of exposure of the modified electrode to the oxygen plasma was varied from 10 to 60 min. Based on IR spectra of the ITO|npSG before and after exposure to the activated oxygen gas, a treatment time of 20 min was selected. Under these conditions, the amide-II stretching band from the dendrimer at 1550 cm^{-1} [20] was eliminated, and the band at 1644 cm^{-1} , which results from a combination of H-O-H deformation and amide-I stretching from the dendrimer, was shifted to 1634 cm^{-1} , the expected position for a band that is due exclusively to H-O-H stretching (Fig. 1). The typical peaks for Si-O-Si due to the asymmetric stretching at $1000\text{--}1100\text{ cm}^{-1}$, symmetric stretching at 799 cm^{-1} , and bending at $400\text{--}500\text{ cm}^{-1}$ [21–23] were retained.

Because of the limited sensitivity of the IR measurements, only attenuation of the amount of PAMAM is demonstrated by the results in Fig. 1. Evidence for the diminution of PAMAM to a level inconsequential to this study was obtained by cyclic voltammetry of $\text{Fe}(\text{CN})_6^{3-}$ at an ITO|npSG electrode (Fig. 2). Prior to treatment with the oxygen plasma, the shape of the current-potential curve was distorted, probably by interaction of the protonated amines of the PAMAM with the $\text{Fe}(\text{CN})_6^{3-}$. After exposure to the oxygen plasma, the shape of the voltammogram approached that for a reversible, one-electron process that is not complicated by adsorption or a coupled reaction. At $20\text{ mV}\cdot\text{s}^{-1}$ the difference in peak potentials, ΔE_p , was 80 mV and the ratio of the anodic-to-cathodic peak current was 0.98. Although ΔE_p was greater than the expected value, 59 mV, for a reversible, one-electron process, it agreed with that observed for the voltammetry of $\text{Fe}(\text{CN})_6^{3-}$ at an electrode modified in the same manner except for excluding PAMAM from the precursor solution. The peak currents were increased, albeit by less than 10%, at the electrode after oxygen plasma treatment, a result attributed to a change in pore volume. A role of PAMAM in determining the pore size of the npSG that is electrochemically deposited is indicated by comparing the peak current for the reduction of $\text{Fe}(\text{CN})_6^{3-}$ at an electrode prepared as in Fig. 2 (with PAMAM removed by plasma treatment) to an electrode fabricated by an identical procedure except for absence of PAMAM in the precursor solution. The peak currents with the former electrode were 30% greater at $20\text{ mV}\cdot\text{s}^{-1}$ than those at the latter electrode, which suggests an increase in pore size when PAMAM is included in the sol-gel precursor solution. An alternative explanation for this increase in peak current is that the post-deposition treatment may have damaged the film. Scanning electron microscopy was used to evaluate the integrity of the film (Fig. 3). There is no evidence of ablation or cracking of the silica film. The oxygen-plasma treatment was used in all subsequent experiments.

3.2. Voltammetry of 5-HTPP at ITO modified with a sol-gel film of controlled porosity

Prior to studying the oxidation of 5-HTPP at ITO|npSG, cyclic voltammetry of this compound in aqueous solution at pH 7.2 (phosphate buffer) was performed with bare glassy carbon and bare ITO electrodes. A well-defined oxidation peak at 0.4 V at glassy carbon electrode was observed, whereas at bare ITO, 5-HTPP shows an oxidation peak at 0.8 V. The difference between the oxidation peak potential at GC and ITO is similar to that reported in a study of a related compound, 5-hydroxytryptamine, in which the respective values were 0.40 V and 0.65 V [24]. The cause of this potential shift is not known but probably relates to a difference in the double layer structure and/or the surface chemistry of

the analytes at carbon and oxide electrodes. Attempts to investigate the cyclic voltammetry of 5-HTPP as a function of scan rate at bare ITO were not successful because of passivation of the electrode surface. That is, the anodic current at 0.8 V decreased with scan number. After 20 scans at $50 \text{ mV}\cdot\text{s}^{-1}$ in pH 7.2 phosphate buffer, the current is 40% of its initial value. Passivation of the electrode during the oxidation of 5-HTPP [14,15,25] and of related compounds, 5-hydroxytryptamine and tryptophan [25], was reported previously. It probably resulted from the accumulation of polymeric products on the surface [15,25,26]. Indeed, a hypothesis of the present study is that by restricting the oxidation to the nanopore domain, passivation will be mitigated by sterically decreasing polymerization [9,10]. An adsorbed dione film was produced at pH 7.5 at a pyrolytic graphite electrode, but rather than causing passivation, this film was conductive [27]. Indeed, the dione film mediated the oxidation of NADH [26]. In an attempt to circumvent the passivation during continuous cyclic voltammetry of 5-HTPP, a 2-min delay between scans was employed; however, the decrease in current with scan number was still observed. When the experiments were repeated at pH 2.6, the same general trend was seen.

In contrast to the above result, the current for the oxidation of 5-HTPP ($1.0 \times 10^{-4} \text{ M}$) at an ITO|npSG electrode persisted during continuous scanning (Fig. 4a). There was an 8% decrease from the initial anodic current at 0.8 V during the first three cycles, but after 17 additional cycles, the anodic peak current was only 11% lower than that of the initial value. Moreover, incorporating a delay time of 2 min between each cycle retained the current at its initial value (Fig. 4b), suggesting that partial depletion of 5-HTPP in the pores of the sol-gel film was the reason for the observed decrease in current at an ITO|npSG electrode when a delay between scans was not employed (Fig. 4a). Repeating the interrupted-scan experiment in Fig. 4b but with a pH 2.6 electrolyte also resulted in an absence of passivation of the ITO|npSG electrode. Chronoamperometry in stirred solution yielded a stable current for the oxidation of 5-HTPP at ITO|npSG. Increasing the concentration of 5-HTPP in $2.0 \mu\text{M}$ increments (10 additions over a 700 s period) yielded a plot where the current increase with final addition was only 5% lower than that for the first addition. That the ITO|npSG electrode is not passivated during the voltammetry of 5-HTPP under conditions where voltammetry at bare ITO loses activity was hypothesized to result from a change in the pathway of the oxidation of 5-HTPP when this reaction occurs in the spatially restricted environment of the nanoscale pores. That is, the formation of polymeric species from the electrochemically generated cation radical is apparently suppressed in npSG. This observation is consistent with previous studies on the oxidation of aniline in silica sol-gel matrices [9,10]. In these studies, when the silica was processed into the microporous domain, the oxidation of aniline yielded dimers and small oligomers, whereas with mesoporous silica, polyaniline was formed [9,10].

Experimental evidence that the pathway of the oxidation of 5-HTPP at ITO was changed by the npSG film was obtained by controlled potential electrolysis followed by mass spectroscopy of the products in the electrolyte. At ITO and ITO|npSG electrodes, 30-min electrolyses at 1.0 V were performed on $20 \mu\text{M}$ 5-HTPP in 0.1 M KCl (adjusted to pH 2.6 with HCl) and in 0.1 M phosphate buffer (pH 7.2). The major products in the electrolyte were identified by MALDI-TOF mass spectrometry. Here, $10 \mu\text{L}$ of the electrolyzed solution was mixed with $10 \mu\text{L}$ of saturated CHCA prepared in a 1:1 (volume) mixture of water and acetonitrile. Aliquots ($1.0 \mu\text{L}$) of the mixture were dried on the MALDI sample holder. The results are shown in Fig. 5. The known peaks for the matrix at m/z 191 and 380 served as calibration points [13]. When the electrolyses were performed at bare ITO, the major products were tryptophan-4,5-dione, the C-C coupled dimer (5,5'-dihydroxy-4,4'-bitryptophan), and the oxygen-bridged dimer, which have peaks at m/z 236, 440, and 455, respectively. The peak at m/z 220 in Fig. 5 is due to unreacted 5-HTPP. When the results obtained for electrolyses at pH 2.6 and 7.2 were compared, it was noted that the

abundance of the dione relative to the dimers was greater at pH 2.6 than at pH 7.2. These results are comparable to those reported for electrolyses at a pyrolytic graphite electrode (PGE) except that at a PGE the oxygen-linked dimer was not significant at pH 2.6 [25,28].

The electrolyses were repeated but with an ITO|npSG electrode. The mass spectra (Fig. 6) illustrated that dimers were the primary products in the electrolyte at both pH 2.6 and 7.2; that is, a peak for tryptophan-4,5-dione was absent at both pH values. These results support the hypothesis that the npSG film on the electrode results in a change of the oxidation pathway. Apparently, the nanoscale domain in which the radical cation of 5-HTPP is formed causes its local concentration to be sufficient to favor the dimerization reaction. This conjecture is consistent with the report that if the carbo-cation radical, which is the initial product of the oxidation of 5-HTPP, is adsorbed on a given electrode, dimerization occurs [25]. For the present study, an important result is that at ITO|npSG passivation does not occur, which suggests that polymerization is not a factor. In our previous report on aniline oxidation in pores of monolithic sol-gels [9], the absence of polymerization was attributed to steric factor related to the nm-scale pore size. Finally, tryptophan-4,5-dione was not seen in the mass spectrometry of the electrolysis products when ITO|npSG was the working electrode. The data do not preclude formation of the dione in that it may be deposited on the electrode as a non-passivating film. In this regard, only aliquots from the electrolyzed liquid phase served as samples in the mass spectrometry.

Because the oxidation of 5-HTPP at ITO|npSG electrodes occurred without passivation, a diagnosis of the current-limiting factor was feasible. A $\log v$ versus $\log i_p$ plot (v , scan rate; i_p , peak current) was obtained for the oxidation of 1.0×10^{-4} M 5-HTPP over the range, 20 – 100 $\text{mV}\cdot\text{s}^{-1}$ in 0.1 M phosphate buffer (pH 7.2). A linear least squares fit of the data yielded a slope of 0.39 and $R^2 = 0.997$. The slope is less the theoretical value, 0.50, for current limited by linear diffusion. A combination of hemispherical diffusion to the interface of the SG and the bulk solution and linear diffusion through the pores of the SG will yield a slope in the range 0.0 – 0.5, but considering the film thickness (estimated as 100 nm by scanning electron microscopy across the edge of the SG) and the scan rates employed, this possibility was discounted. A probable cause of the slope below 0.5 in this experiment is a peak current that is partially limited by kinetics of the electron-transfer reaction.

For analytical applications, diffusion-limited currents are preferred over kinetic currents in that they yield linear calibration curves and greater sensitivity. To obtain an electrode that both eliminates passivation and yields a diffusion-limited oxidation of 5-HTPP, the ITO|npSG was modified with cobalt hexacyanoferrate (CoHCF), as described in the Experimental section. The selection of CoHCF was based reports that it has been synthesized in sol-gels [19,29,30] and that it has served as a catalyst for the oxidation of related compounds, particularly L-tryptophan [16,31–35]. Sequential immersion of ITO|npSG in 0.01 M CoCl_2 and in 0.01 M $\text{K}_3\text{Fe}(\text{CN})_6$ was used to prepare CoHCF.

Spectroscopic evidence for its formation was obtained by reflectance UV-visible spectrophotometry, which showed the ligand-to-metal charge transfer at 385 nm and the high-spin d-d transition of Co^{II} at 600 nm that are characteristic of this compound [19]. The infrared spectrum had peaks at 2105 cm^{-1} and 2085 cm^{-1} ; they have been attributed to $\text{Fe}^{\text{II}}\text{-CN-Co}^{\text{II}}$ stretching [36]. In addition, the cyclic voltammetry of the modified ITO|npSG in phosphate buffer (pH 7.2) was comparable to that of a film of CoHCF on a glassy carbon electrode in a pH 7.0 phosphate buffer [34].

The cyclic voltammetry of 5-HTPP in pH 7.2 phosphate buffer at ITO|npSG (Fig. 3) and at ITO|npSG|CoHCF electrodes was compared. The presence of CoHCF decreased the potential for the oxidation by 280 mV. The oxidation of 5-HTPP at 0.52 V is apparently by a

mediated process that is initiated by the electrochemical oxidation of CoHCF at that potential. In this regard, CoHCF exhibited electrocatalysis via mediation of electron transfer in a study on the oxidation of dopamine [37]. The peak current for the oxidation of 5-HTPP at ITO|npSG|CoHCF at 0.52 V was greater than the current for this oxidation at ITO|npSG at 0.8 V. Assuming that the effective areas of the electrode in Fig. 3 and the ITO|npSG|CoHCF electrode are the same, the observed augmentation of the current suggests that rate of the electron-transfer reaction via the mediated pathway is greater than that for direct electrochemical oxidation of 5-HTPP. This interpretation is supported by a study of the current-limiting process at ITO|npSG|CoHCF. A $\log v$ versus $\log i_p$ plot was obtained for the oxidation of 1.0×10^{-4} M 5-HTPP over the range, 20 – 100 $\text{mV}\cdot\text{s}^{-1}$ in 0.1 M phosphate buffer (pH 7.2). Linear least squares fit of the data yielded a slope of 0.48 and R^2 of 0.997. The agreement with the theoretical slope, 0.5, demonstrates that the current is limited by linear diffusion. While a change from kinetic to diffusion control accounts for some of the increase in peak current, the presence of CoHCF undoubtedly increases the effective area of the working electrode relative to that of ITO|npSG.

3.3. Flow injection amperometric determination of 5-HTPP at ITO modified with a sol-gel film of controlled porosity

The analytical utility of the ITO|npSG|CoHCF electrode for the determination of 5-HTPP was evaluated by linear scan voltammetry and by flow-injection analysis (FIA) with detection by amperometry at constant applied potential. With linear scan voltammetry (50 $\text{mV}\cdot\text{s}^{-1}$) at ITO|npSG|CoHCF in 0.1 M phosphate buffer (pH 7.2), the current at 0.52 V increased linearly with 5-HTPP concentration over the range from 10 μM to 1.0 mM. A linear least squares fit of the data yielded a slope of $0.06 \mu\text{A}\cdot\mu\text{M}^{-1}$ and R^2 of 0.996 ($n = 8$). The detection limit was 2.1 μM using the criterion of the concentration that gives a signal of 3-times the uncertainty, which was taken as the standard deviation of a set of five replicates on a 10 μM sample. With FIA, data were obtained at concentrations down to 0.20 μM 5-HTPP; a set of replicate trials is shown in Fig. 7. A calibration curve was obtained over the concentration range, 0.50 – 60 μM 5-HTPP (Fig. 8). The experimental conditions were the following: applied potential, 1.0 V; carrier solution, 0.1 M phosphate buffer (pH 7.2); injection volume, 100 μL ; and flow rate, 2.5 $\text{mL}\cdot\text{min}^{-1}$. Linear least squares fit of the data (9 points) yielded the following: slope, $0.085 \mu\text{A}\cdot\mu\text{M}^{-1}$, y-intercept, 18 nA; and R^2 , 0.999. Fifteen replicate trials on a 0.20 μM 5-HTPP had a peak current of $0.036 \pm 0.001 \mu\text{A}$, which gave a detection limit ($k = 3$ criterion) of 17 nM. Electrodes modified with an electron-transfer mediator are not selective in that any analyte that is oxidized by the mediator will give a signal. Therefore, such electrodes need to be employed in an electrochemical detector coupled to a separation method such as HPLC for practical application in the determination of mixtures.

4. Conclusions

A method for the electrochemically assisted deposition of a ca. 100-nm sol-gel film with porosity controlled by inclusion of a surfactant, CTAB, and generation-4 poly(amidoamine) dendrimer, PAMAM, is reported. The removal of the PAMAM and CTAB by treatment with an oxygen plasma and by extraction with an alcohol resulted in a pore structure that permitted facile diffusion of ionic test species such as hexacyanoferrate therein. Moreover, this mesoporous sol-gel film on an ITO electrode protected the surface from passivation during the oxidation of 5-HTPP. The anodic process, which occurs in the nanoscale pores of the film, forms a cation radical. In this spatially restricted environment, polymerization that will lead to deposition of a passivating film on a bare electrode does not occur. Using mass spectrometry of the supporting electrolyte after controlled potential electrolysis, carbon-linked and oxygen-linked dimers were identified as the primary products of oxidation at the

modified electrode. Cyclic voltammetry as a function of scan rate showed that the current at this electrode was limited in part by the kinetics of the electron-transfer reaction. When the ITO surface is further modified by formation of cobalt hexacyanoferrate, the mediated oxidation of 5-HTPP is observed. In this case, the current in cyclic voltammetry over scan rates in the range, 20 – 100 mV·s⁻¹, is limited by linear diffusion, a process that results in a peak current proportional to concentration.

This electrode design is intended to serve as an amperometric detector for analytes that can form passivating products via chemical reactions coupled to charge transfer and/or for measurements in matrices that contain surface-active macromolecules. In the latter case, the controlled pore structure is projected to block diffusion of such matrix components to the electrode surface. It is assumed that the sol-gel in either its present state or in a modified form will not become coated with such matrix elements. The promise of this application is demonstrated in the present study by FIA with amperometric detection for the determination of 5-HTPP in the concentration range, 0.50 – 60 μM. A detection limit, k = 3 criterion, of 17 nM was attained.

Acknowledgments

This study was supported in part by the U.S. National Institutes of Health through grant R15GM087662-01 to J.A.C. The study was performed in part at Miami University where D.R. was a Visiting Scholar on leave from the School of Advanced Studies of the University of Camerino.

References

1. Sittampalam G, Wilson GS. *Anal Chem.* 1983; 55:1608–1610.
2. Wandstrat MM, Spindel WU, Pacey GE, Cox JA. *Electroanalysis.* 2007; 19:139–143.
3. Walcarius A, Sibottier E, Etienne M, Ghanbaja J. *Nat Mater.* 2007; 6:602–608. [PubMed: 17589513]
4. Shacham R, Avnir D, Mandler D. *Adv Mater.* 1999; 11:384–388.
5. Shacham R, Mandler D, Avnir D. *Chem - Eur J.* 2004; 10:1936–1943.
6. Shacham R, Avnir D, Mandler D. *J Sol-Gel Sci Technol.* 2004; 31:329–334.
7. Ohira A, Ishizaki T, Sakata M, Taniguchi I, Hirayama C, Kunitake M. *Colloids Surf A.* 2000; 169:27–33.
8. Tess ME, Cox JA. *Electroanalysis.* 1998; 10:1237–1240.
9. Widera J, Cox JA. *Electrochem Commun.* 2002; 4:118–122.
10. Widera J, Kijak AM, Ca DV, Pacey GE, Taylor RT, Perfect H, Cox JA. *Electrochim Acta.* 2005; 50:1703–1709.
11. Tess ME, Cox JA. *J Electroanal Chem.* 1998; 457:163–169.
12. Ueda M, Kim HB, Ikeda T, Ichimura I. *Chem Mater.* 1992; 4:1229–1233.
13. Cohen JL, Cox JA. *J Sol-Gel Sci Technol.* 2003; 28:15–18.
14. Cohen JL, Cox JA. *J Solid State Electrochem.* 2004; 8:886–891.
15. Cohen JL, Widera J, Cox JA. *Electroanalysis.* 2002; 14:231–234.
16. Liu Y, Xu L. *Sensors.* 2007; 7:2446–2457.
17. Hierlemann A, Campbell JK, Baker LA, Crooks RM, Ricco AJ. *J Am Chem Soc.* 1998; 120:5323.
18. Li J, Piehler T, Qin D, Baker JR Jr, Tomalia DA. *Langmuir.* 2000; 16:5613.
19. Zamponi S, Giorgetti M, Berrettoni M, Kulesza PJ, Cox JA, Kijak AM. *Electrochim Acta.* 2005; 51:118–124.
20. Garcia ME, Baker LA, Crooks RM. *Anal Chem.* 1999; 71:256–258. [PubMed: 21662946]
21. Karmakar B, De G, Ganguli D. *J Non-Cryst Solids.* 2000; 272:119–126.
22. De G, Karmakar B, Ganguli D. *J Mater Chem.* 2000; 10:2289–2293.
23. Zhang X, Wu Y, He S, Yang D. *Surf Coat Technol.* 2007; 201:6051–6058.

24. Goyal RN, Oyama M, Gupta VK, Singh SP, Sharma RS. *Sens Actuators B*. 2008; 134:816–821.
25. Humphries KA, Wrona MZ, Dryhurst G. *J Electroanal Chem*. 1993; 346:377–403.
26. Hoyer B, Jensen N. *J Electroanal Chem*. 2007; 601:153–160.
27. de-los-Santos-Alvarez N, Lobo-Castanon MJ, Miranda-Ordieres AJ, Tunon-Blanco P, Abruna HD. *Anal Chem*. 2005; 77:2624–2631. [PubMed: 15828802]
28. Humphries K, Dryhurst G. *J Pharm Sci*. 1987; 76:839–847. [PubMed: 3501464]
29. Ca DV, Cox JA. *Microchim Acta*. 2004; 147:31–37.
30. Moore JG, Lochner EJ, Ramsey C, Dalal NS, Stiegman AE. *Angew Chem Int Ed*. 2003; 42:2741–2743.
31. Cai CX, Xue KH, Xu SM. *J Electroanal Chem*. 2000; 486:111–118.
32. Golabi SM, Noor-Mohammadi F. *J Solid State Electrochem*. 1998; 2:30–37.
33. Cai CX, Ju HX, Chen HY. *J Electroanal Chem*. 1995; 397:185–190.
34. Xun ZY, Cai CX, Xing W, Lu TH. *J Electroanal Chem*. 2003; 545:19–27.
35. Chen SM. *Electrochim Acta*. 1998; 43:3359–3369.
36. Sato O, Einaga Y, Fujishima A, Hashimoto K. *Inorg Chem*. 1998; 38:4405–4412. [PubMed: 11671150]
37. Shi LH, Wu T, Wang MJ, Li D, Zhang YJ, Li JH. *Chin J Chem*. 2005; 23:149–154.

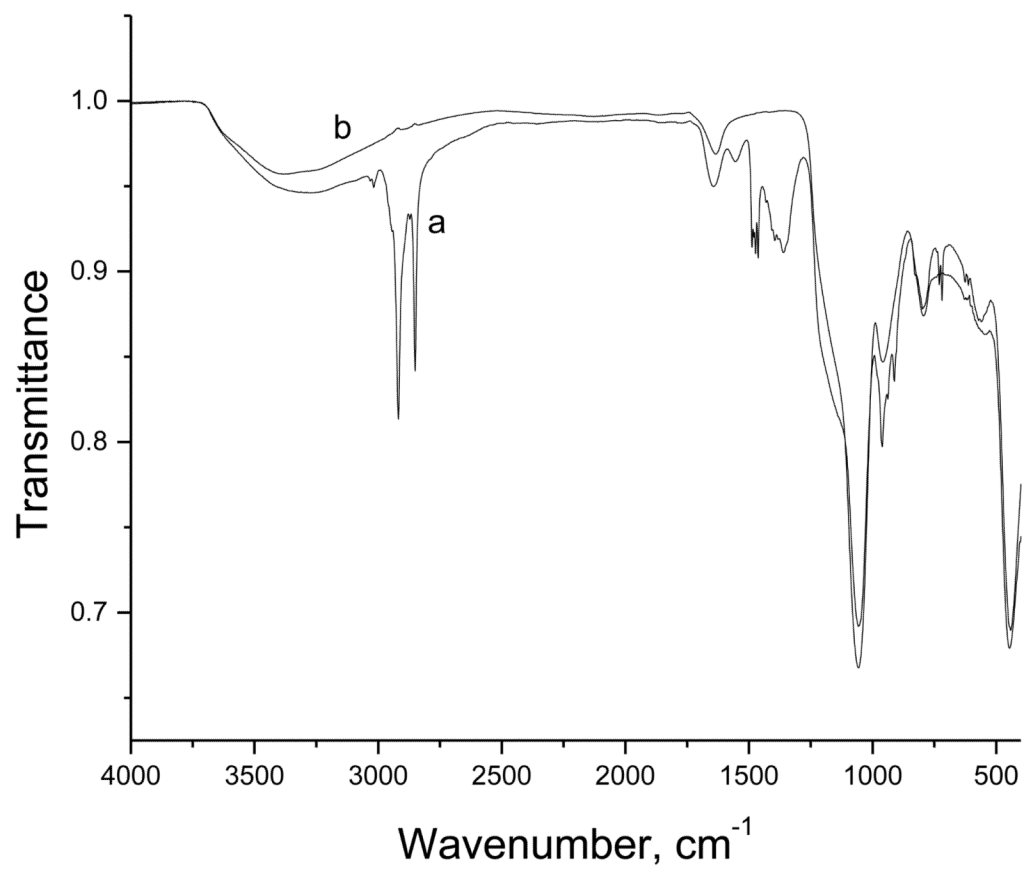


Fig. 1. IR spectra before (a) and after (b) oxygen plasma treatment of ITO|npSG electrode.

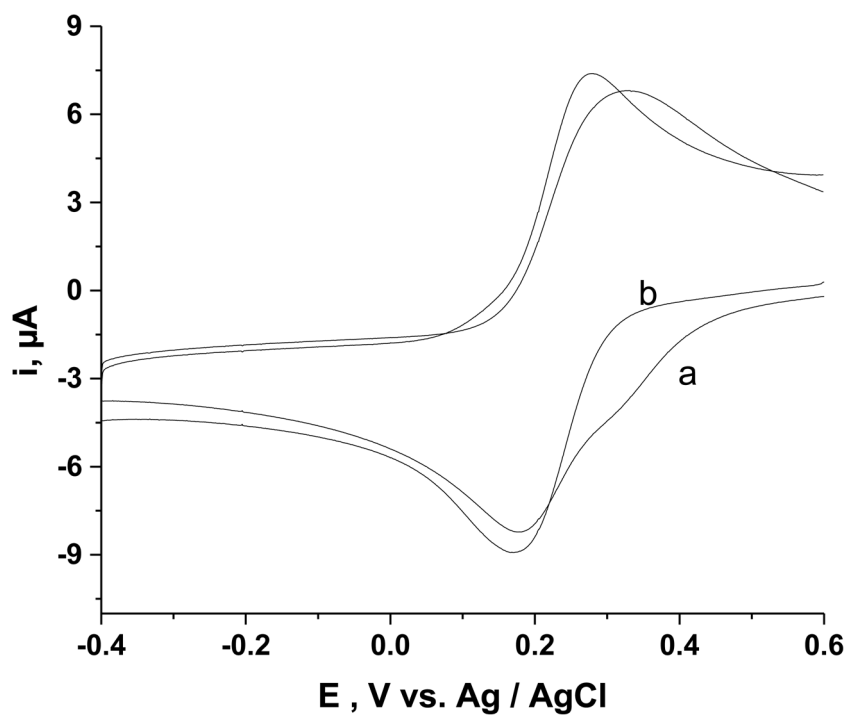


Fig.2. Cyclic voltammetry of 1.0 mM $\text{K}_3\text{Fe}(\text{CN})_6$ at an ITO|npSG electrode before (a) and after (b) oxygen plasma treatment. Electrolyte 0.1 M KCl; scan rate $50 \text{ mV}\cdot\text{s}^{-1}$.

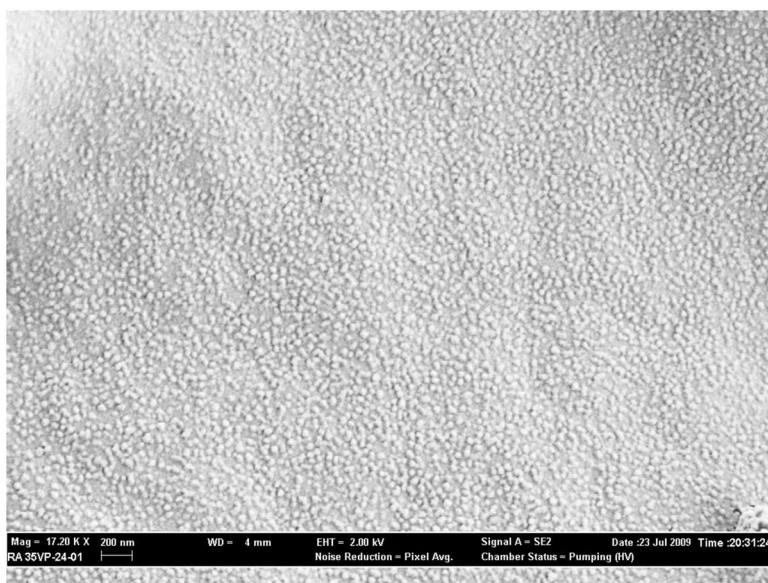


Fig. 3. Scanning electron microscopy image of ITO/npSG after a 20-min treatment with an oxygen plasma operated at 100 Watts and 0.3 Torr.

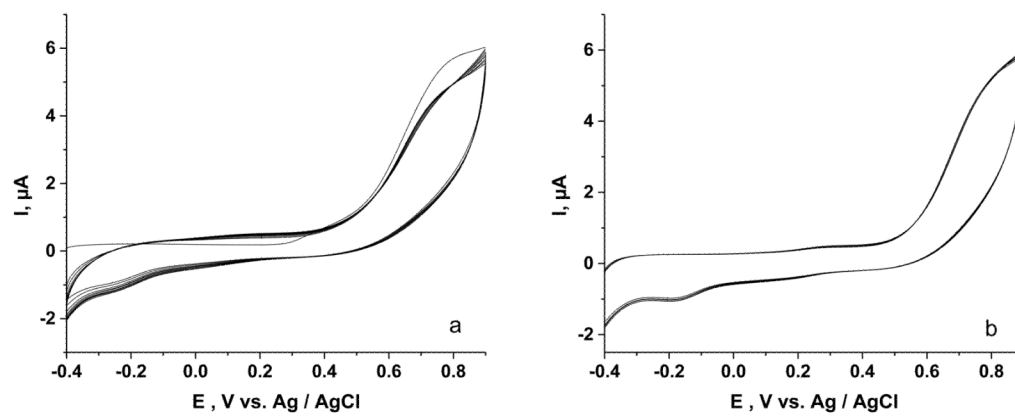


Fig. 4. Cyclic voltammetry of 1.0×10^{-4} M 5-HTPP at an ITO|npSG in 0.1 M phosphate buffer (pH 7.2), Scan rate $50 \text{ mV} \cdot \text{s}^{-1}$. a) Twenty continuous cycles; b) Twenty cycles with a 2-min delay between each scan.

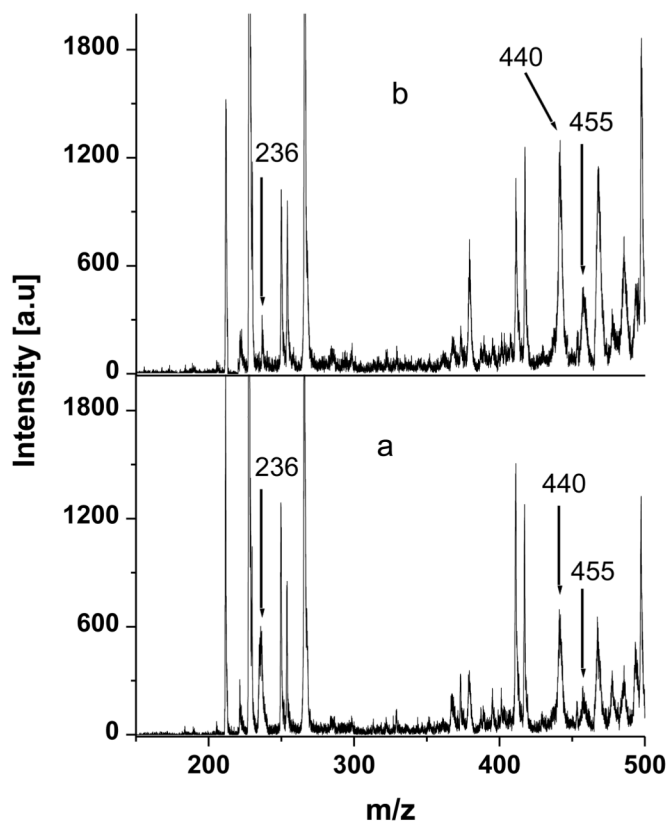


Fig. 5. MALDI-TOF mass spectrum of the supporting electrolyte after controlled potential oxidation of 20 μM 5-HTPP at bare ITO electrode. Supporting electrolyte, a) 0.1 M KCl (adjusted to pH 2.6 with HCl); b) 0.1 M phosphate buffer (pH 7.2).

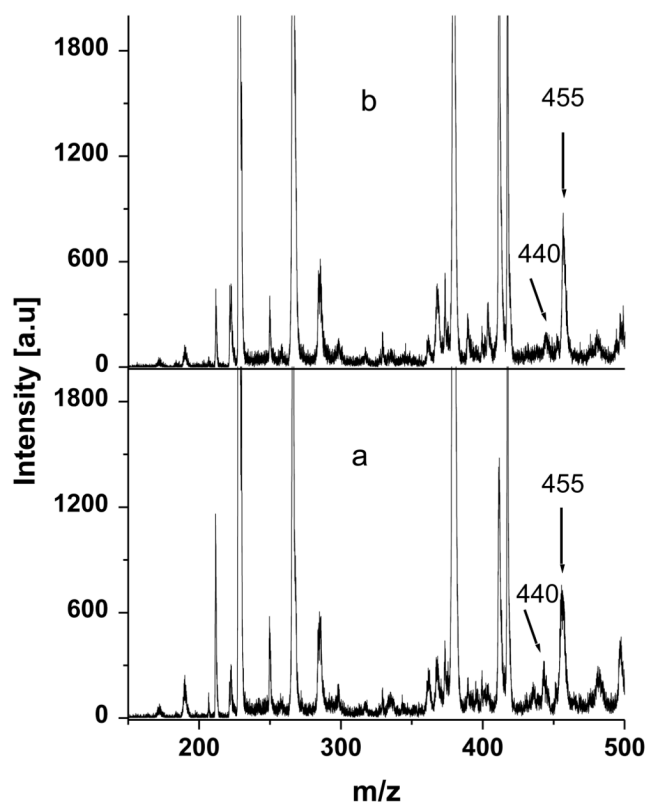


Fig. 6. MALDI-TOF mass spectrum after controlled potential oxidation of 20 μM 5-HTPP at an ITO|npSG electrode. Supporting electrolyte, a) 0.1 M KCl (adjusted to pH 2.6 with HCl); b) 0.1 M phosphate buffer (pH 7.2).

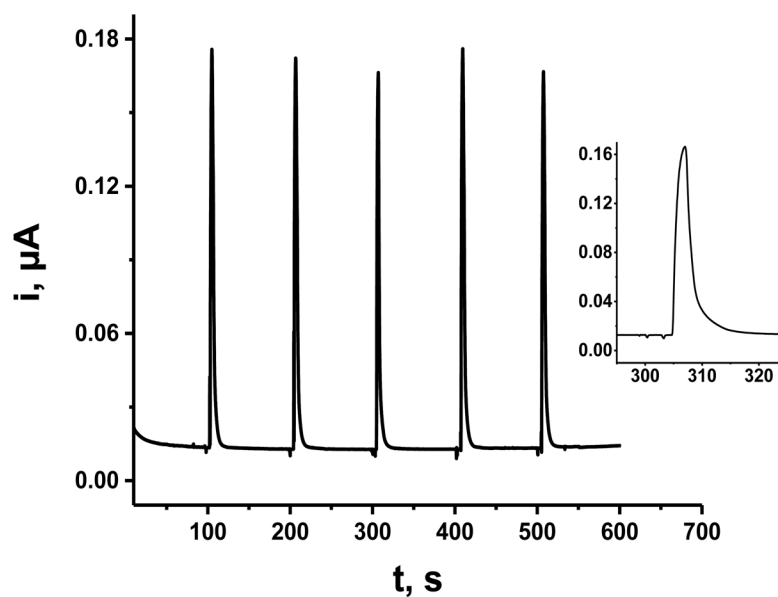


Fig. 7. Replicate trials of flow-injection amperometry of 2.0 μM 5-HTPP at an ITO|npSG|CoHCF electrode. Carrier solution, 0.1 M phosphate buffer (pH 7.2); flow rate 2.5 mL min^{-1} ; 5-HTPP concentration, 2.0 μM ; potential, +1.0 V; injection volume, 100 μL . The inset shows the magnified version of a single peak.

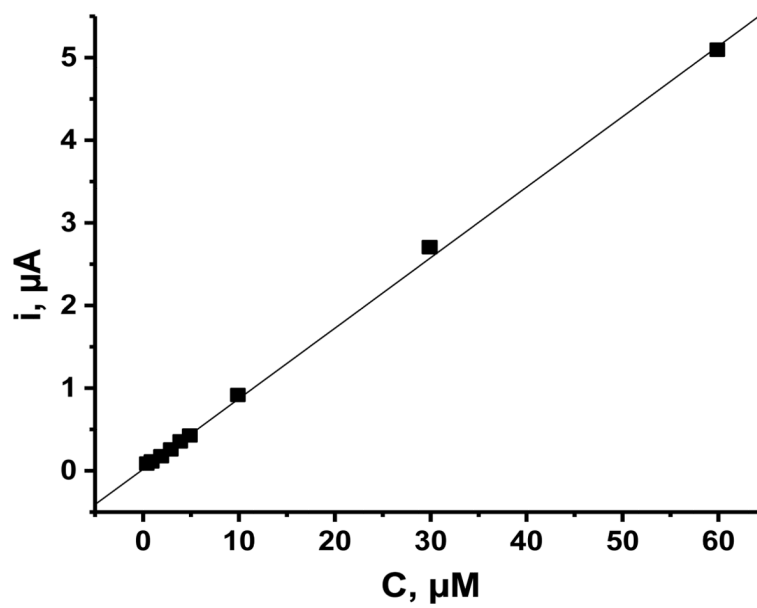


Fig. 8. Calibration curve for the flow-injection amperometric determination of 5-HTPP at an ITO|npSG|CoHCF electrode. The conditions are those in Fig. 7.